A&A 382, 282–290 (2002)
DOI: 10.1051/0004-6361:20011621

Astronomy & Astrophysics

Study of electron density in planetary nebulae

A comparison of different density indicators

M. V. F. Copetti[1,2] and B. C. Writzl[1]

[1] Laboratório de Análise Numérica e Astrofísica, Departamento de Matemática, Universidade Federal de Santa Maria, 97119-900 Santa Maria, RS, Brazil
[2] Physics Department, University of Cincinnati, Cincinnati OH 45221-0011, USA

Received 29 August 2001 / Accepted 7 November 2001

Abstract. We present a comparison of electron density estimates for planetary nebulae based on different emission-line ratios. We have considered the density indicators [O II]λ3729/λ3726, [S II]λ6716/λ6731, [Cl III]λ5517/λ5537, [Ar IV]λ4711/λ4740, C III]λ1906/λ1909 and [N I]λ5202/λ5199. The observational data were extracted from the literature. We have found systematic deviations from the density homogeneous models, in the sense that: $N_{\rm e}$(N I) $\lesssim$ $N_{\rm e}$(O II) $<$ $N_{\rm e}$(S II, C III, Cl III or Ar IV) and $N_{\rm e}$(S II) $\approx$ $N_{\rm e}$(C III) $\approx$ $N_{\rm e}$(Cl III) $\approx$ $N_{\rm e}$(Ar IV). We argue that the lower [O II] density estimates are likely due to errors in the atomic parameters used.

Key words. ISM: planetary nebulae

1. Introduction

The electron density, $N_{\rm e}$, is one of the key physical parameters needed to characterise a planetary nebula. Some density assessment is necessary to confidently derive the chemical abundance of the nebula, to calculate the total mass of ionised gas and is even useful to estimate the distance of the object. Most of the density estimates found in the literature are based on measurements of a single emission-line ratio sensitive to it obtained from spectra taken from special areas of the nebulae, usually the brightest ones. In the presence of internal variations of electron density, these single line ratio measurements may not be representative of all ionising zones. In fact, the analysis by Stanghellini & Kaler (1989) of a large data sample of planetary nebulae taken from the literature have indicated the existence of statistically significant discrepancies between the values of electron densities obtained from distinct density sensors as [O II]λ3729/λ3726, [S II]λ6716/λ6731, [Cl III]λ5517/λ5537, [Ar IV]λ4711/λ4740. In special, they have found [S II] densities generally higher than those from [O II]. However, Kingsburgh & English (1992), using their own homogeneous data for 63 galactic planetary nebulae, have found densities derived from integrated [O II] and [S II] doublet ratios in excellent agreement with each other. On the other hand, Meatheringham & Dopita (1991), for a sample of 44 planetary nebulae in the Magellanic Clouds, have found the opposite, i.e., [O II] densities systematically higher than [S II] ones. More recently, Keenan et al. (1996, 1997, 1999), based on data from the series of high spectral resolution observations of planetary nebulae by Hyung, Aller and collaborators (see references in Sect. 2), have made simultaneous determinations of electron density and temperature from different ratios of [S II], [Ar IV] and [O II] optical and ultraviolet emission-lines and have found them to be in excellent internal consistency and in generally good agreement with values obtained from sensors associated to different ions. In the present paper we readdress the subject of comparing the electron density estimated from different ions.

Send offprint requests to: M. V. F. Copetti,
e-mail: mvfc@lana.ccne.ufsm.br

2. Analysis

The data used were taken from the electronic emission-line catalogue for planetary nebulae by Kaler et al. (1997), from Kingsburgh & English (1992) and from the spectral survey of high surface brightness planetaries by Hyung, Aller, Feibelman and collaborators (Aller & Hyung 1995; Aller et al. 1996; Feibelman et al. 1994, 1996; Hyung 1994; Hyung & Aller 1995a,b, 1996, 1997a,b, 1998; Hyung et al. 1993, 1994a,b,c, 1995, 1997, 1999a,b, 2000, 2001; Keyes et al. 1990). Instead of comparing directly the derived densities, as has been done by other authors, what implies in discarding all line ratios close or beyond the saturation limits at low and high densities, we have compared the line ratios themselves with one another.

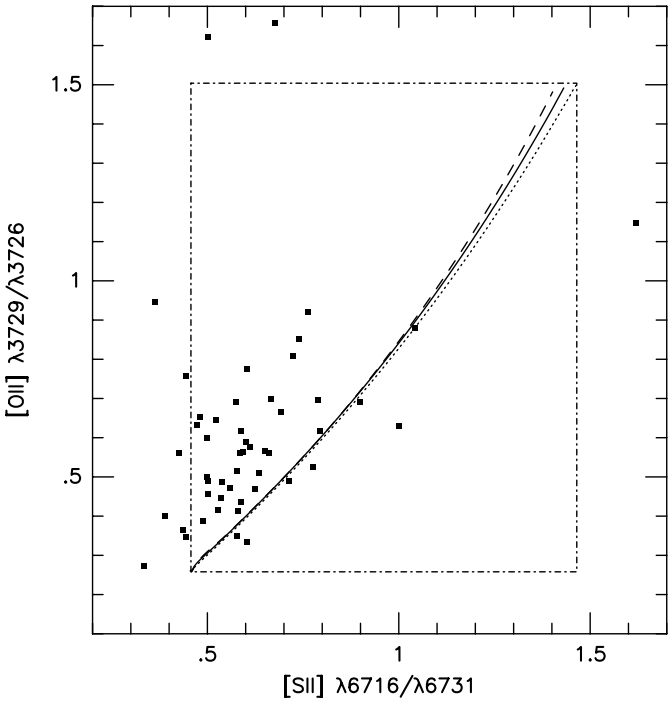

Fig. 1. [S II]λ6716/λ6731 vs. [O II]λ3729/λ3726 for the same nebular region data from Kaler et al. The dotted, solid and dashed lines are the *loci* of density homogeneous nebulae at electron temperatures of 5000, 10 000 and 15 000 K, respectively. On these curves, the density increases from the top-right to the bottom-left. The dotted-dashed rectangle shows the low and high density saturation limits of these line ratios.

Three kinds of analyses were done with the data from the catalogue of Kaler et al. (1997). First, for each comparison, we have selected the data for those objects that had the respective pair of emission line ratios measured on a same area or section of the nebula and taken from a same bibliographic source. These data from a common nebular region should better cope with the possible internal electron density variations. However, in some cases the number of objects selected was very small or even null, as for the comparisons with C III]λ1906/λ1909. For the second kind of analysis we have calculated the standard deviations and the mean values of the line ratios for each planetary nebula (regardless of the area from where the data were obtained). For single measurements ratios we arbitrarily attributed the value of 20% of the mean to the standard deviation. A large spread of the data was found in these two kinds of comparisons with points falling far beyond the saturation limits of the respective line ratios (e.g. Figs. 1 and 2). In fact in many cases no correlation between the density indicator ratios is perceived. The same problem is also seen in some of the Stanghellini & Kaler (1989) plots. Part of the data spread is genuine and reflects the internal variation of density in the nebulae. On the other hand, the data have came from a variety of sources and have different accuracies and some may be unreliable. Therefore in the third kind of analysis we have selected a most homogeneous sub-sample of the mean data. For the comparison of the [S II], [S II] and [Cl III] ratios we have selected those data with the standard deviations, σ, of less than 15% of the mean and for the [Ar IV] ratio we increase this limit to 20%. For the other density indicator, the small number of data did not allow this sample selection. With this procedure we have discarded the single measurements and the objects with strong density variations.

Table 1. References for the atomic data.

ion	n	ion. potential (eV)		references	
X^i		X^{i-1}	X^i	coll. str.	trans. prob.
N I	5	00.0	14.5	[1, 2]	[3, 4]
S II	8	10.4	23.4	[5]	[6, 7]
O II	5	13.6	35.1	[8, 9]	[4]
Cl III	5	23.8	39.9	[10]	[3, 11]
C III	5	24.4	47.9	[12]	[4, 13, 14]
Ar IV	5	40.9	59.8	[15]	[3, 16]

References: [1] Pequignot & Aldrovandi (1976); [2] Dopita et al. (1976); [3] Kaufman & Sugar (1986); [4] Wiese et al. (1996); [5] Ramsbottom et al. (1996); [6] Verner et al. (1996); [7] Keenan et al. (1993); [8] Pradhan (1976); [9] McLaughlin & Bell (1993); [10] Butler & Zeippen (1989); [11] Mendoza (1983); [12] Berrington et al. (1985) (extrapolated to $T_e = 5000$ K); [13] Glass (1983); [14] Nussbaumer & Storey (1978); [15] Zeippen et al. (1987); [16] Mendoza & Zeippen (1982).

3. Results

In Figs. 1–17 we have shown the comparisons of the density indicator [Ar IV] λ4711/λ4740, [Cl III] λ5517/λ5537, [O II] λ3729/λ3726, [S II] λ6716/λ6731, C III] λ1906/λ1909 and [N I] λ5202/λ5199 to one another. As the three analyses mentioned in Sect. 2 of the data from the catalogue by Kaler et al. (1997) have shown the same trends in all cases, we have presented here only the best plot available for each comparison with the exception of the [S II] vs. [O II] comparison for which all plots are shown as example. In all these figures, the lines are the *loci* of density homogeneous nebulae at different electron temperatures and the rectangle delimitates the space of allowed values for these line ratios between the low and high density limits. The theoretical calculations have been done with the n-levels atom programme *temden* contained in the *nebular STSDAS/IRAF* package (see Shaw & Dufour 1995). The references for the collision strengths and transition probabilities used are listed in Table 1 together with the number of levels n considered and the ionization potentials of the ion and of its predecessor.

In the following, the results of the comparisons are discussed.

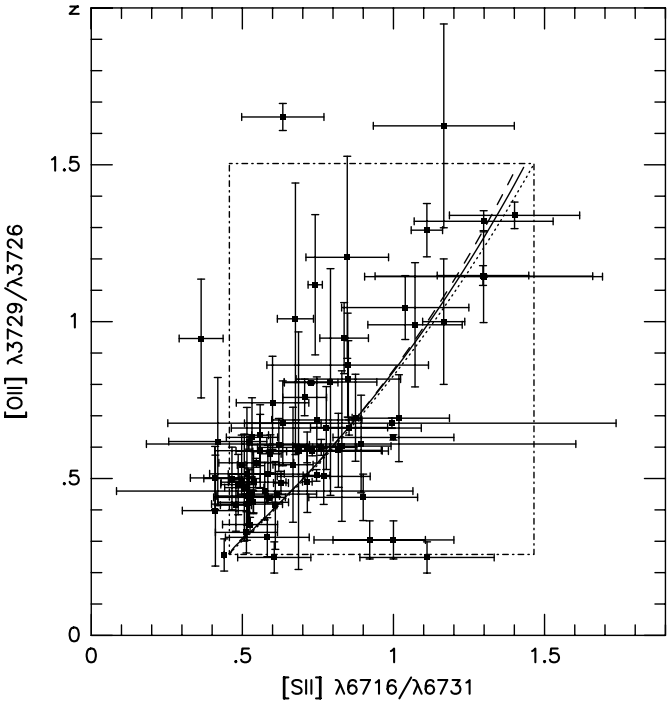

Fig. 2. [S II]λ6716/λ6731 vs. [O II]λ3729/λ3726 for the mean values for the whole sample from Kaler et al. The error bars are the standard deviations of the respective line ratios. Lines as in Fig. 1.

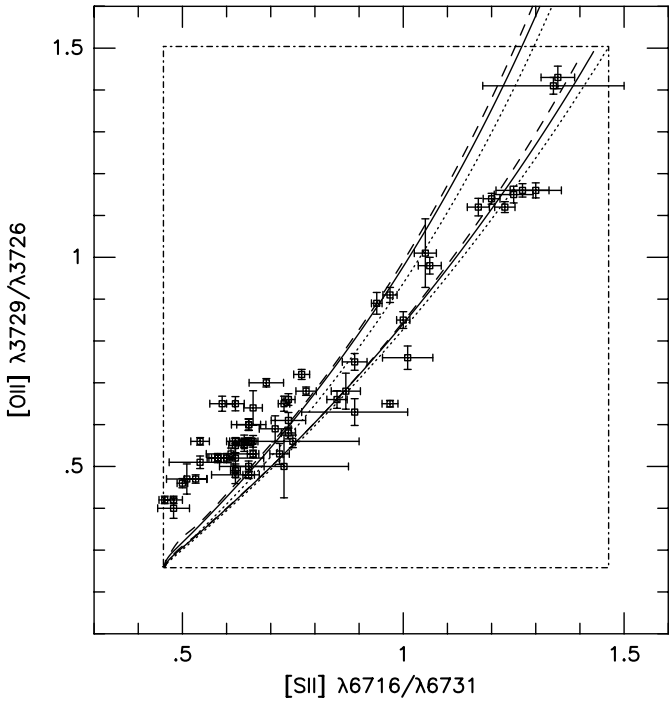

Fig. 4. [S II]λ6716/λ6731 vs. [O II]λ3729/λ3726 for the data from Kingsburgh & English (1992). Lines as in Fig. 1. For the upper set of models the collision strenghts from McLaughlin & Bell (1998) were adopted.

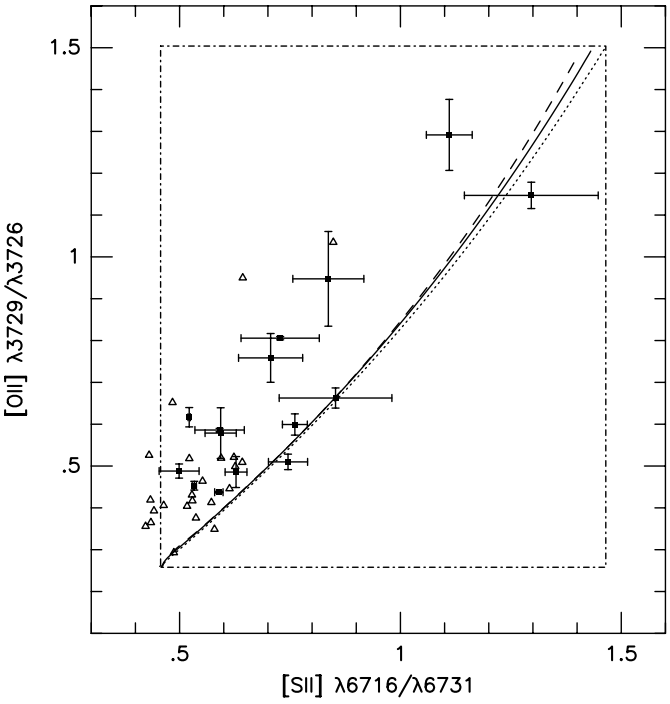

Fig. 3. [S II]λ6716/λ6731 vs. [O II]λ3729/λ3726. Data: (■) mean values for the selected sample ($\sigma < 15\%$) from Kaler et al. (from left to right: NGC 6644, NGC 6741, NGC 6884, IC 4846, IC 1747, IC 2165, NGC 6210, NGC 40, Me 2-1, IC 351, NGC 6818, NGC 6445, IC 4593, NGC 650 and NGC 6853); (△) from Hyung, Aller and collaborators. Lines as in Fig. 1.

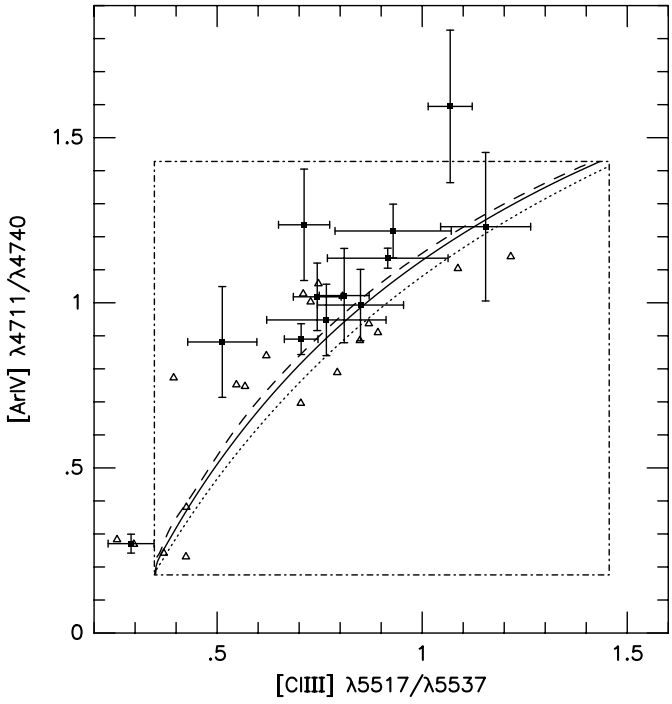

Fig. 5. [Cl III]λ5517/λ5537 vs. [Ar IV]λ4711/λ4740. Data: (■) mean values for the selected sample ($\sigma < 15\%$) from Kaler et al. (from left to right: NGC 7027, NGC 6886, NGC 6884, Hu 1-2, IC 5217, NGC 6210, IC 2165, NGC 2440, IC 2003, NGC 3242, Me 2-1 and NGC 2022); (△) from Hyung, Aller and collaborators. Lines as in Figs. 1.

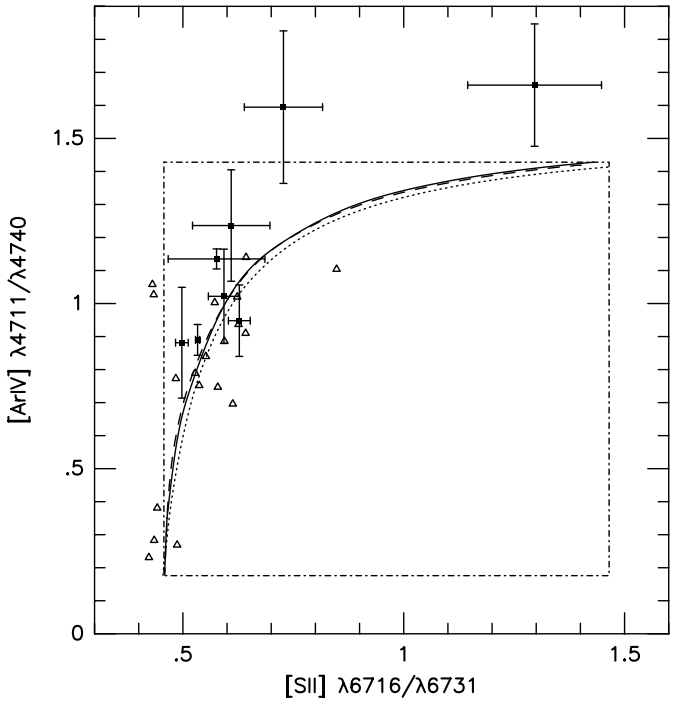

Fig. 6. [S II]λ6716/λ6731 vs. [Ar IV]λ4711/λ4740. Data: (■) mean values for the selected sample ($\sigma < 20\%$) from Kaler et al. (from left to right: NGC 6886, NGC 6884, IC 2003, IC 2165, Hu 1-2, NGC 6210, Me 2-1 and NGC 6853); (△) from Hyung, Aller and collaborators. Lines as in Fig. 1.

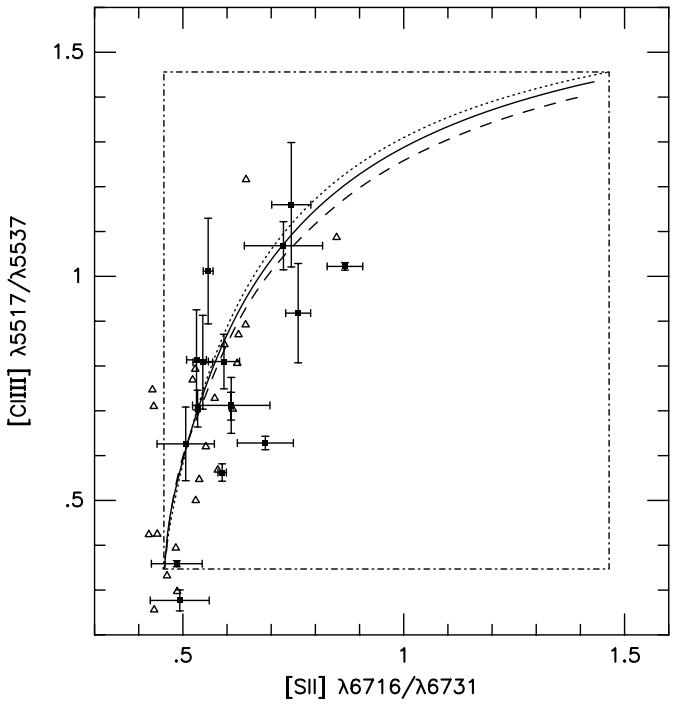

Fig. 7. [S II]λ6716/λ6731 vs. [Cl III]λ5517/λ5537. Data: (■) mean values for the selected sample ($\sigma < 15\%$) from Kaler et al. (from left to right: M 1-74, IC 5117, NGC 6567, NGC 6153, NGC 6884, NGC 6578, M 1-17, IC 4846, IC 2165, Hb 12, Hu 1-2, NGC 2867, Me 2-1, IC 351, NGC 6818 and NGC 6778); (△) from Hyung, Aller and collaborators. Lines as in Fig. 1.

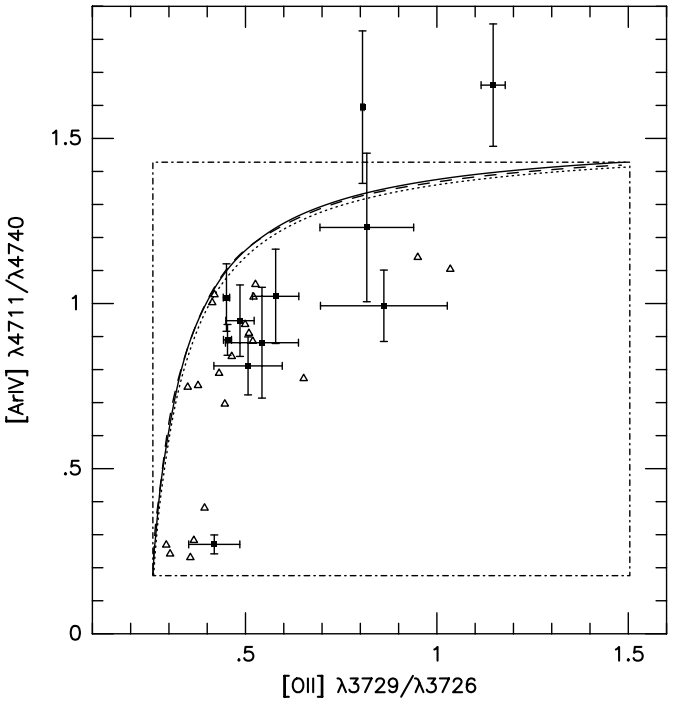

Fig. 8. [O II]λ3729/λ3726 vs. [Ar IV]λ4711/λ4740. Data: (■) mean values for the selected sample ($\sigma < 20\%$) from Kaler et al. (from left to right: NGC 7027, IC 5217, NGC 6884, NGC 6210, NGC 6803, NGC 6886, IC 2165, Me 2-1, NGC 2022, NGC 2440 and NGC 6853); (△) from Hyung, Aller and collaborators. Lines as in Fig. 1.

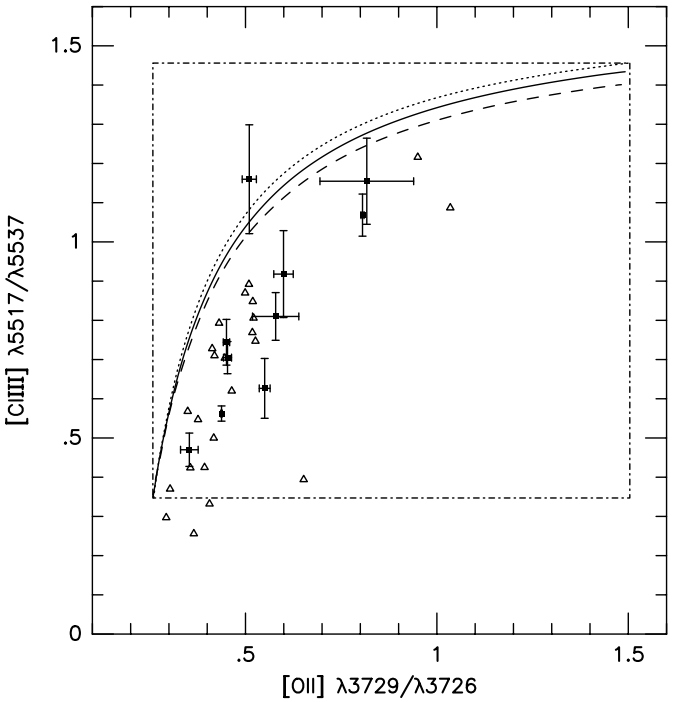

Fig. 9. [O II]λ3729/λ3726 vs. [Cl III]λ5517/λ5537. Data: (■) mean values for the selected sample ($\sigma < 15\%$) from Kaler et al. (from left to right: IC 4997, IC 4846, IC 5217, NGC 6884, IC 351, Cn 3-1, IC 2165, NGC 6818, Me 2-1 and NGC 2022); (△) from Hyung, Aller and collaborators. Lines as in Fig. 1.

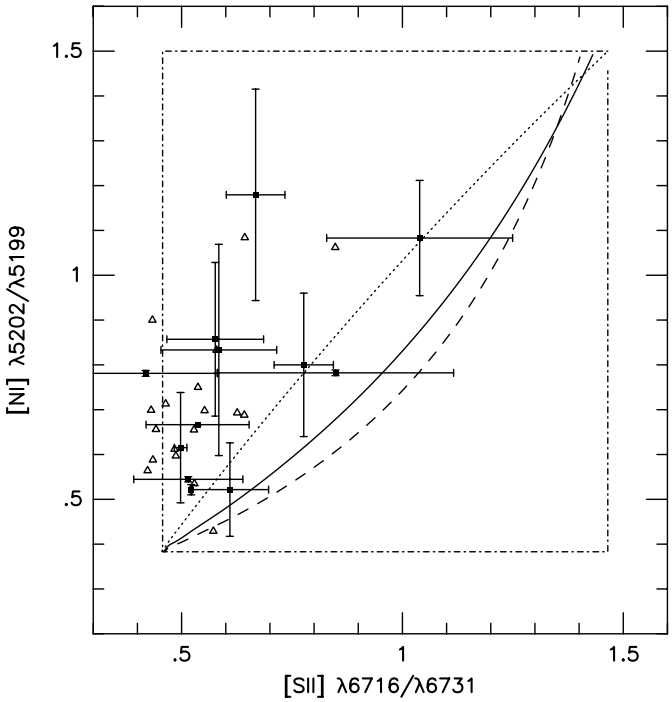

Fig. 10. [S II]λ6716/λ6731 vs. [N I]λ5202/λ5199. Data: (■) mean values for the whole sample from Kaler et al. (from left to right: NGC 6302, NGC 6886, IC 418, NGC 6741, NGC 6572, IC 2003, NGC 7009, Hu 1-2, NGC 6309, NGC 6543, Hu 1-1, NGC 2440 and NGC 6720); (△) from Hyung, Aller and collaborators. Lines as in Fig. 1.

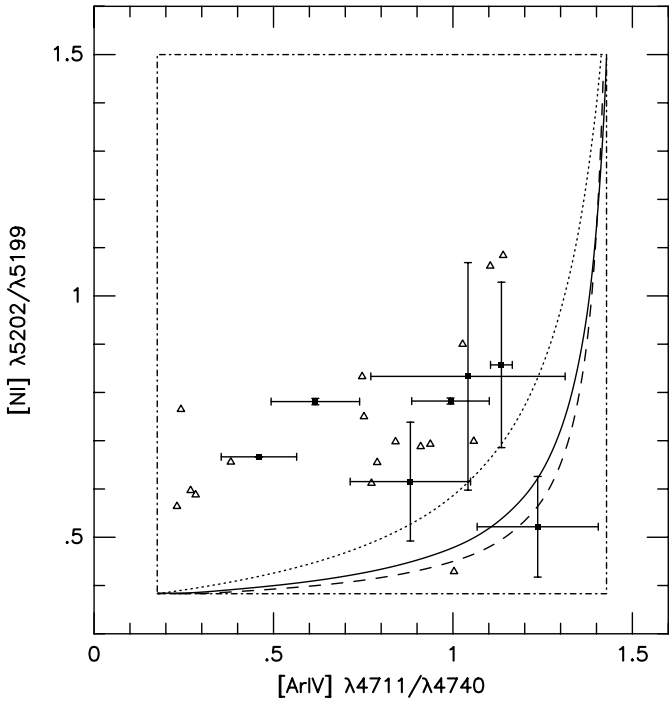

Fig. 12. [Ar IV]λ4711/λ4740 vs. [N I]λ5202/λ5199. Data: (■) mean values for the whole sample from Kaler et al. (from left to right: NGC 6572, NGC 6302, NGC 6886, NGC 2440, NGC 7009, IC 2003 and Hu 1-2); (△) from Hyung, Aller and collaborators. Lines as in Fig. 1.

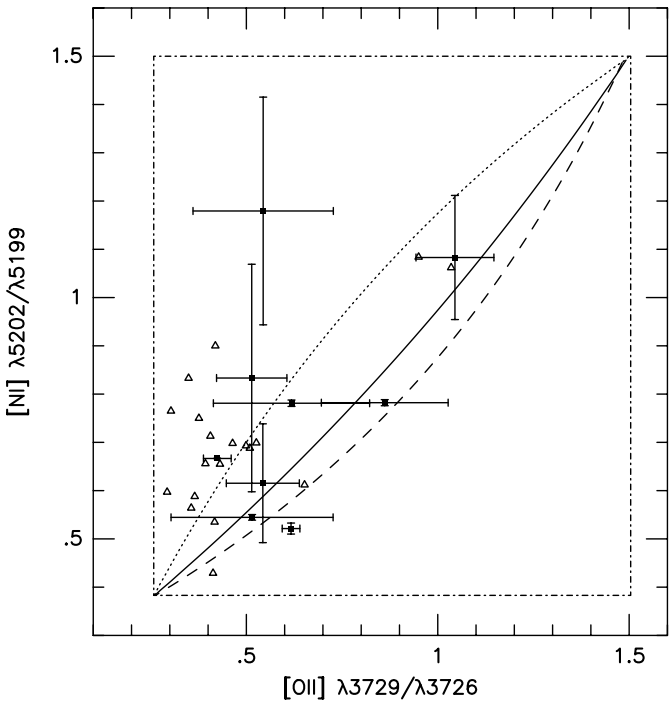

Fig. 11. [O II]λ3729/λ3726 vs. [N I]λ5202/λ5199. Data: (■) mean values for the whole sample from Kaler et al. (from left to right: NGC 6572, NGC 7009, IC 418, NGC 6886, NGC 6309, NGC 6741, NGC 6302, NGC 2440 and NGC 6720); (△) from Hyung, Aller and collaborators. Lines as in Fig. 1.

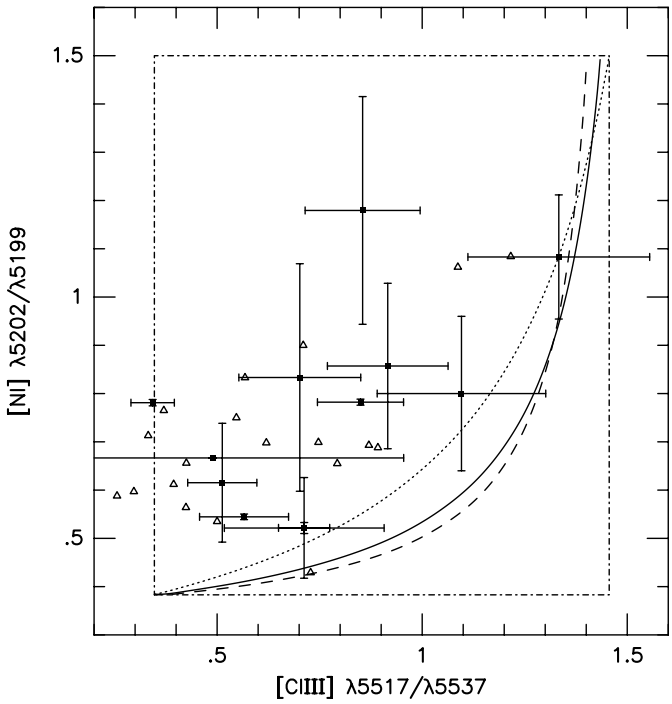

Fig. 13. [Cl III]λ5517/λ5537 vs. [N I]λ5202/λ5199. Data: (■) mean values for the whole sample from Kaler et al. (from left to right: NGC 6302, NGC 6572, NGC 6886, IC 418, NGC 7009, Hu 1-2, NGC 6741, NGC 2440, NGC 6309, IC 2003, Hu 1-1 and NGC 6720); (△) from Hyung, Aller and collaborators. Lines as in Fig. 1.

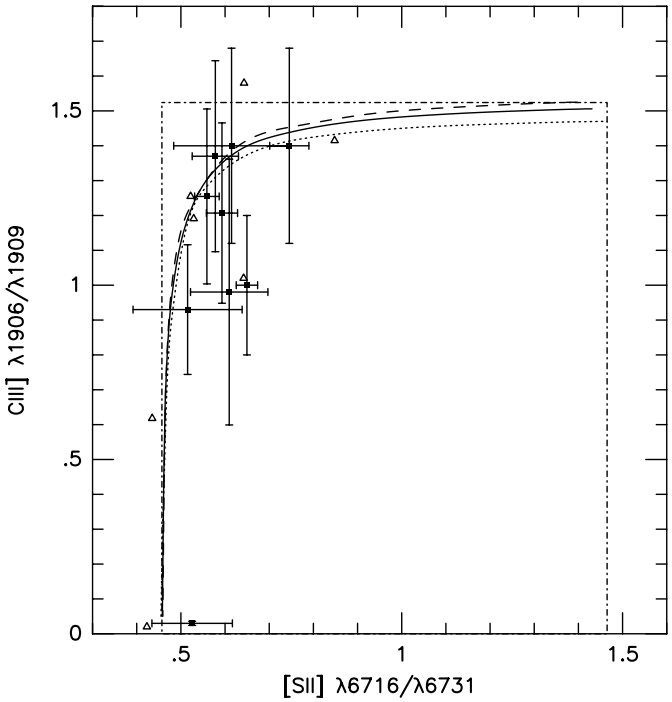

Fig. 14. [S II]λ6716/λ6731 vs. C III]λ1906/λ1909. Data: (■) mean values for the whole sample from Kaler et al. (from left to right: IC 418, IC 4997, IC 2149, J 900, IC 2165, Hu 1-2, IC 5217, IC 1297 and IC 351); (△) from Hyung, Aller and collaborators. Lines as in Fig. 1.

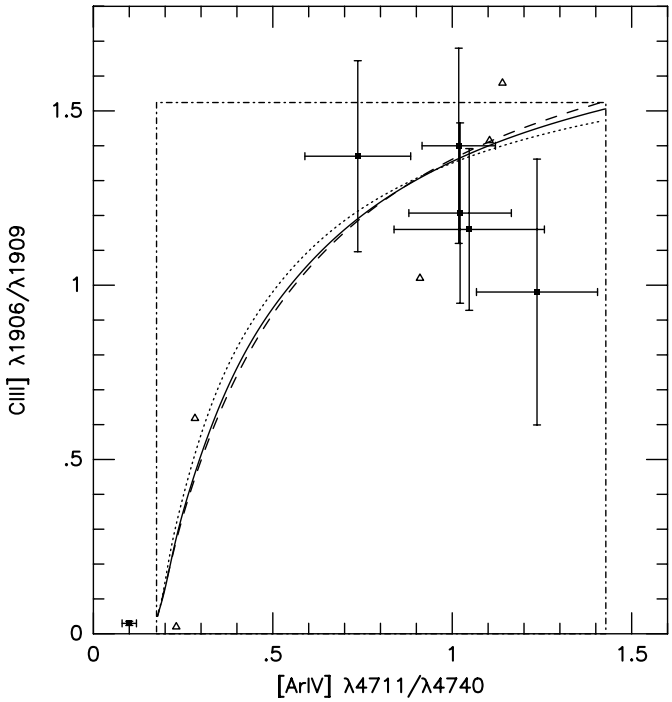

Fig. 16. [Ar IV]λ4711/λ4740 vs. C III]λ1906/λ1909. Data: (■) mean values for the whole sample from Kaler et al. (from left to right: IC 4997, J 900, IC 5217, IC 2165, IC 3568 and Hu 1-2); (△) from Hyung, Aller and collaborators. Lines as in Fig. 1.

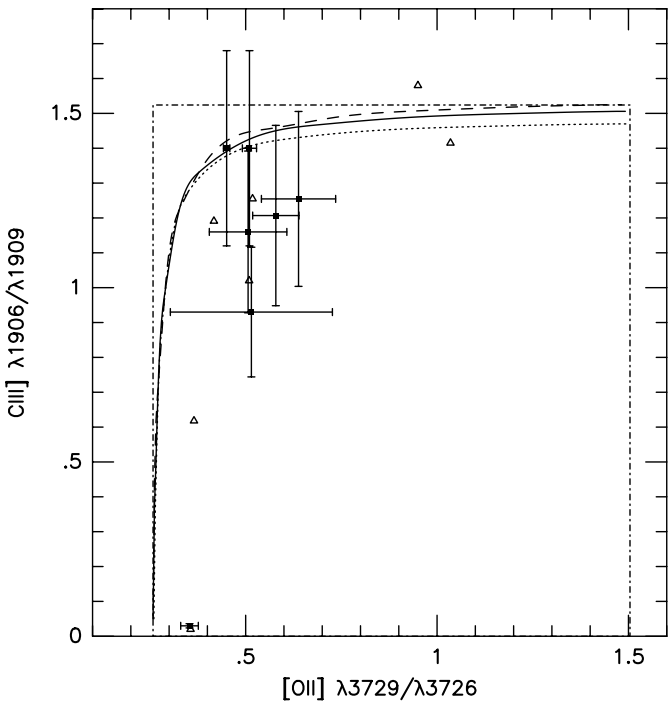

Fig. 15. [O II]λ3729/λ3726 vs. C III]λ1906/λ1909. Data: (■) mean values for the whole sample from Kaler et al. (from left to right: IC 4997, IC 5217, IC 3568, IC 351, IC 418, IC 2165 and IC 2149); (△) from Hyung, Aller and collaborators. Lines as in Fig. 1.

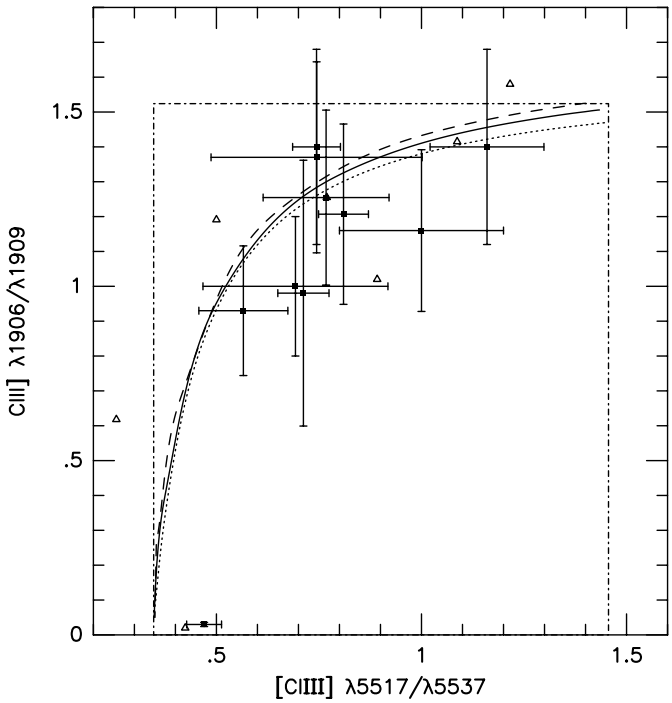

Fig. 17. [Cl III]λ5517/λ5537 vs. C III]λ1906/λ1909. Data: (■) mean values for the whole sample from Kaler et al. (from left to right: IC 4997, IC 418, IC 1297, Hu 1-2, IC 5217, J 900, IC 2149, IC 2165, IC 3568 and IC 351); (△) from Hyung, Aller and collaborators. Lines as in Fig. 1.

3.1. [S II] vs. [O II]

Figures 1 and 2 show the comparison between [S II] and [O II] density sensors for the same region data and for the mean data from Kaler et al. (1997), respectively. In Fig. 3 we have the same comparison for the mean ratios for the selected sample from the Kaler et al. and for the data from Hyung, Aller and collaborators as well. For Fig. 4 we have used the homogeneous data from Kingsburgh & English (1992) which is missing in the Kaler et al. (1997) catalogue. These plots clearly indicate that the [S II] electron density estimates are statistically higher than the [O II] ones for the densest nebulae. The data from Meatheringham & Dopita (1991), who have claimed the opposite, were already in the Kaler et al. catalogue and are included in our plots. The fact that Kingsburgh & English (1992) and Keenan et al. (1996, 1999) have not found any discrepancy between the densities derived from the [O II] and [S II] ratios demonstrates that the direct comparison between the density sensor is a better approach for this aim. Due to the non linear conversion from line ratio to electron density specially near to the saturation limits any discrepancy between different density estimates tends to be hidden by the large errors in density.

It is important to consider that we are assuming a same electron temperature for the S II and O II zones. As can be seen in Figs. 1–4, the theoretical relationship between [S II] and [O II] ratios is very weakly dependent on the adopted electron temperature in the case of homogeneous models. Although we could shift the middle section of these curves adopting different temperatures in each zones, both ends are virtually tight, specially on the high density limit, where the density sensors are independent on the temperature. So the discrepancy between [S II] and [O II] densities near the high density limit is certainly not an effect of the adopted electron temperatures.

Arguably two sequences can be perceived in Figs. 3 and 4: one following closely the density homogeneous models and the other with $N_{\rm e}({\rm S\,II}) > N_{\rm e}({\rm O\,II})$. Interestingly, Phillips (1998) has found that the relationship nebular radius versus [S II] density has two distinct branches with a discontinuity in densities at nebular radius close to 0.1 pc. To explain this discontinuity Phillips has proposed that most planetary nebulae contain two primary [S II] emission zones, with densities differing approximately by a factor of 10^2. The dominant component for the emission would be dependent on evolutionary state of the nebula. It would be valuable to know whether or not a similar discontinuity is also found in [O II] densities.

In the past, [S II] densities on average several times higher than those derived from the [O II] ratio had been found (Aller & Epps 1976; Saraph & Seaton 1970). However, most of this difference was accounted on errors in atomic parameters used. In fact, the calibration of electron density with the [S II] $\lambda 6716/\lambda 6731$ line ratio have changed significantly over the years. For instance, according to Saraph & Seaton (1970), at an electron temperature of 10 000 K, [S II] $\lambda 6716/\lambda 6731 = 1$ would correspond to $N_{\rm e} = 2200$ cm^{-3}, while the current evaluation would be of $N_{\rm e} = 610$ cm^{-3}. More recently, Stanghellini & Kaler (1989) have found $N_{\rm e}({\rm S\,II})$ higher than $N_{\rm e}({\rm O\,II})$ by only 5% or 16%, depending on the data selection. Rubin (1989) has suggested that [S II] densities higher than those from [O II] may be caused by a dynamical "plow effect" at the ionising front, which would increase the density of the matter just beyond the H^+ edge.

It is not unreasonable to expect that the remaining discrepancy between the [S II] and [O II] density estimates was still caused by errors in the atomic parameters, although since the compilation of atomic parameters relevant to nebular diagnostics by Mendoza (1983) till few years ago only slight shifts towards the opposite direction had been verified in the calibrations of these density sensors with an increase of the densities derived from [S II] and a decrease of those from [O II] within the linear sections of these calibrations. More recently, Keenan et al. (1999) have shown that the calculations of [O II] collision strengths by McLaughlin & Bell (1998) have a striking effect on the theoretical [O II] ratio specially at low electron densities. However, as can be seen in Fig. 4, the adoption of the atomic data of McLaughlin & Bell (1998) would not make a significative difference in the high density range and would bring an additional problem for the lower density range, since the models calculated using the collision strengths of Pradhan (1976) fit much better the observational data from Kingsburgh & English (1992).

We think that the discrepancy between the [S II] and [O II] density estimates is more likely due to uncertainties in the atomic parameters because the fraction of the S^+ ionization zone outside the O^+ zone should be very small at least for a nebula limited by radiation. The fact that at the low density limit the [S II] and [O II] ratios are in first approximation dependent only on the relative values of the statistical weights of the upper levels of these transitions would explain why the compatibility between the data and the models is higher for the less dense objects. At the high density limit the spontaneous transition probabilities are the dominant parameters and both these line ratios are given by

$$r = \frac{3}{2} A(^2{\rm D}_{5/2} - {}^4{\rm S}_{3/2}) / A(^2{\rm D}_{3/2} - {}^4{\rm S}_{3/2}) \text{ as } N_{\rm e} \to \infty.$$

Although there are some points in Figs. 3 and 4 reaching the [S II] high density limit, none of the best measurements of the [O II] ratio is close to its predicted high density limit $r = 0.26$. This fact could be indicating that the transition probabilities for the O II ion should be revised. A 25–50% increase in the above transition probability ratio for the O II ion would result in much better compatibility between the models and observations. Interestingly, not long ago, the opposite situation was prevailing with the theoretical [O II] ratio higher the observed value (see Zeippen 1987).

3.2. [Ar IV] and [Cl III]

The ratio [Ar IV]λ4711/λ4740 is a density sensor for the innermost parts of the nebula. Observationally, high resolution is required to resolve [Ar IV] λ4711 from the He I λ4713 line and measure accurately the doublet. Probably due to the contaminations of the He I line, a large scatter in measurements of the [Ar IV] lines is found in the Kaler et al. (1997) catalogue with a fair quantity of data corresponding to [Ar IV] ratios well above the low density limit. Our selection procedure have eliminated most of them. However, as the [Ar IV] lines are only strong in high excitation nebulae, only a small number of data passed the selection.

The comparison between the [Ar IV] and [Cl III] ratios is shown in Fig. 5. The data for these ions are fairly compatible with the homogeneous models. Figures 6–9 show the comparisons of these two density sensor with the [S II] and [O II] ratios. The [S II] densities are consistent with those derived from the [Ar IV] and [Cl III] ratios, whereas the [O II] ratio definitely indicates lower densities. It is important to realize that, as can be inferred from the values of the ionization potentials (see Table 1), the S^+ zone is basically disjointed of the both the Ar^{+++} and Cl^{++} zones. In contrast, the O^+ and Cl^{++} coexist in a considerable volume of the nebula. Moreover, the S^+ and Cl^{++} zones together encompass the O^+ zone. Therefore, the similarity between [S II] and [Cl III] density estimates and the lower values derived from [O II] are incompatible.

3.3. [N I]

The line ratio [N I]λ5202/λ5199 produces density estimates for the outermost part of the nebula since it is associated to a neutral species with low ionization potential (see Table 1). Relatively few measurements are found for this ratio and it was not considered in the previous comparisons of different density indicators for planetary nebulae (Aller & Epps 1976; Saraph & Seaton 1970; Stanghellini & Kaler 1989). Figures 10–13 show the comparisons of the [N I] ratio with the [S II], [O II], [Ar IV] and [Cl III] ratios for the full object sample from Kaler et al. (1997) and for the data of Hyung, Aller and collaborators. Statistically, the [N I] density estimates are lower or at best marginally compatible with the [O II] ones and definitely lower than those from the [S II], [Ar IV] and [Cl III] ratios.

3.4. C III]

Due to the need of space observations the ultraviolet line ratio C III]λ1906/λ1909 was measured in very few objects. In Figs. 14–17 we have shown the comparisons of this line ratio with the [S II], [O II], [Ar IV] and [Cl III] density sensors for the mean values for the full data sample present in the Kaler et al. (1997) catalogue and the data of Hyung, Aller and collaborators. Within the error bars the C III] densities are compatible with those deduced from the [S II], [Ar IV] and [Cl III] ratios and higher than those derived from the [O II] ratio. In the past C III] densities systematically higher than those from optical ratios had been found (Feibelman et al. 1981) in consequence of errors in the C III] atomic data (Keenan et al. 1992).

4. Conclusions

Based on the atomic data from the references listed in Table 1 and on observational data from the emission-line catalogue for planetary nebulae by Kaler et al. (1997), from Kingsburgh & English (1992) and from the series of high spectral resolution observations of Hyung, Aller and collaborators (see references in Sect. 2), we have found systematic deviations from the density homogeneous models in the comparison of different density indicators, in the sense that:

$$N_{\rm e}({\rm N\,I}) \lesssim N_{\rm e}({\rm O\,II}) < N_{\rm e}({\rm S\,II, C\,III, Cl\,III \text{ or } Ar\,IV}),$$

$$N_{\rm e}({\rm S\,II}) \approx N_{\rm e}({\rm C\,III}) \approx N_{\rm e}({\rm Cl\,III}) \approx N_{\rm e}({\rm Ar\,IV}).$$

Since the same trends were verified in each of the analyses of the data from Kaler et al. (1997) mentioned in Sect. 2 and confirmed with the other two data sets, we are confident that they are not a spurious product of the data selection. Obviously, these results can only have statistical meaning since the planetary nebulae are very inhomogeneous objects.

In principle, some of these discrepancies could be due to possible errors in the atomic parameters needed to derived the electron densities from the line ratios. In fact, most of the discrepancies between density sensors have been eliminated along the years with the improving of the atomic data calculations. In particular, we believe that the [O II] density estimates lower than those derived from the other usual density indicators, the [S II], [Ar IV], [Cl III] and C III] ratios, are likely caused by errors in the [O II] transition probabilities for the following reasons: none of the best measurements of the [O II] ratio reaches the predicted high density limit, as happens with the other ratios; the discrepancy between the [S II] and [O II] densities estimates only occurs near to the high density limit, where the transition probabilities are the key parameters; the dynamical "plow effect" at the ionising front, which would increase the density of the matter just beyond the H^+ edge suggested by Rubin (1989) to explain $N_{\rm e}({\rm N\,II}) > N_{\rm e}({\rm O\,II})$ should have a major impact on the [N I] ratio, the outermost density sensor, and on the contrary the [N I] densities are lower than those derived from the others ratios. Moreover, the [S II] and [Cl III] density estimates are compatible to each other even though the ionizing zones of these two species are distinct. Since these two zones together encompass the O^+ zone, the lower [O II] densities are unexpected. A theoretical reassessment of the O II atomic data and an observational effort to define the [O II] ratio high density limit would be important to clarify the matter.

Acknowledgements. This work was partially supported by the Brazilian institutions CAPES, CNPq and FAPERGS. We thank the anonymous referee for helpful comments and suggestions.

References

Aller, L. H., & Epps, M. W. 1976, ApJ, 204, 445
Aller, L. H., & Hyung, S. 1995, MNRAS, 276, 1101
Aller, L. H., Hyung, S., & Feibelman, W. A. 1996, PASP, 108, 488
Berrington, K. A., Burke, P. G., Dufton, P. L., & Kingston, A. E. 1985, Atom. Data Nucl. Data Tables, 33, 195
Butler, K., & Zeippen, C. J. 1989, A&A, 208, 337
Dopita, M. A., Mason, D. J., & Robb, W. D. 1976, ApJ, 207, 102
Feibelman, W. A., Boggess, A., McCracken, C. W., & Hobbs, R. W. 1981, ApJ, 246, 807
Feibelman, W. A., Hyung, S., & Aller, L. H. 1994, ApJ, 426, 653
Feibelman, W. A., Hyung, S., & Aller, L. H. 1996, MNRAS, 278, 625
Glass, R. 1983, Ap&SS, 92, 307
Hyung, S. 1994, ApJS, 90, 119
Hyung, S., & Aller, L. H. 1995a, MNRAS, 273, 973
Hyung, S., & Aller, L. H. H. 1995b, MNRAS, 273, 958
Hyung, S., & Aller, L. H. 1996, MNRAS, 278, 551
Hyung, S., & Aller, L. H. 1997a, ApJ, 491, 242
Hyung, S., & Aller, L. H. 1997b, MNRAS, 292, 71
Hyung, S., & Aller, L. H. 1998, PASP, 110, 466
Hyung, S., Aller, L. H., & Feibelman, W. A. 1993, PASP, 105, 1279
Hyung, S., Aller, L. H., & Feibelman, W. A. 1994a, MNRAS, 269, 975
Hyung, S., Aller, L. H., & Feibelman, W. A. 1994b, ApJS, 93, 465
Hyung, S., Aller, L. H., & Feibelman, W. A. 1994c, PASP, 106, 745
Hyung, S., Aller, L. H., & Feibelman, W. A. 1997, ApJS, 108, 503
Hyung, S., Aller, L. H., & Feibelman, W. A. 1999a, ApJ, 525, 294
Hyung, S., Aller, L. H., & Feibelman, W. A. 1999b, ApJ, 514, 878
Hyung, S., Aller, L. H., Feibelman, W. A., Lee, W. B., & de Koter, A. 2000, MNRAS, 318, 77
Hyung, S., Aller, L. H., Feibelman, W. A., & Lee, W. 2001, AJ, 122, 954
Hyung, S., Keyes, C. D., & Aller, L. H. 1995, MNRAS, 272, 49
Kaler, J. B., Shaw, R. A., & Browning, L. 1997, PASP, 109, 289
Kaufman, V., & Sugar, J. 1986, J. Phys. Chem. Ref. Data, 15, 321
Keenan, F. P., Feibelman, W. A., & Berrington, K. A. 1992, ApJ, 389, 443
Keenan, F. P., Hibbert, A., Ojha, P. C., & Conlon, E. S. 1993, Phys. Scr., 48, 129
Keenan, F. P., Aller, L. H., Bell, K. L., et al. 1996, MNRAS, 281, 1073
Keenan, F. P., McKenna, F. C., Bell, K. L., et al. 1997, ApJ, 487, 457
Keenan, F. P., Aller, L. H., Bell, K. L., et al. 1999, MNRAS, 304, 27
Keyes, C. D., Aller, L. H., & Feibelman, W. A. 1990, PASP, 102, 59
Kingsburgh, R. L. & English, J. 1992, MNRAS, 259, 635
McLaughlin, B. M., & Bell, K. L. 1993, ApJ, 408, 753
McLaughlin, B. M., & Bell, K. L. 1998, J. Phys. B, 31, 4317
Meatheringham, S. J., & Dopita, M. A. 1991, ApJS, 76, 1085
Mendoza, C., & Zeippen, C. J. 1982, MNRAS, 198, 127
Mendoza, C. 1983, IAU Symp. 103: Planetary Nebulae, 143
Nussbaumer, H., & Storey, P. J. 1978, A&A, 64, 139
Pequignot, D., & Aldrovandi, S. M. V. 1976, A&A, 50, 141
Phillips, J. P. 1998, A&A, 340, 527
Pradhan, A. K. 1976, MNRAS, 177, 31
Rubin, R. H. 1989, ApJS, 69, 897
Ramsbottom, C. A., Bell, K. L., & Stafford, R. P. 1996, Atom. Data Nucl. Data Tables, 63, 57
Shaw, R. A., & Dufour, R. J. 1995, PASP, 107, 896
Saraph, H. E., & Seaton, M. J. 1970, MNRAS, 148, 367
Stanghellini, L., & Kaler, J. B. 1989, ApJ, 343, 811
Verner, D. A., Verner, E. M., & Ferland, G. J. 1996, Atom. Data Nucl. Data Tables, 64, 1
Wiese, W. L., Fuhr, J. R., & Deters, T. M. 1996, Atomic transition probabilities of carbon, nitrogen, and oxygen: a critical data compilation, Washington, Am. Chem. Soc. for the N.I.S.T., 1996
Zeippen, C. J. 1987, A&A, 173, 410
Zeippen, C. J., Le Bourlot, J., & Butler, K. 1987, A&A, 188, 251